POLITECNICO DI TORINO
Repository ISTITUZIONALE

PROGRESS IN MULTI-PHYSICS MODELING OF INNOVATIVE LEAD-COOLED FAST REACTORS

Original
PROGRESS IN MULTI-PHYSICS MODELING OF INNOVATIVE LEAD-COOLED FAST REACTORS / Bonifetto, Roberto; Dulla, Sandra; Ravetto, Piero; Savoldi, Laura; Zanino, Roberto. - In: FUSION SCIENCE AND TECHNOLOGY. - ISSN 1536-1055. - STAMPA. - 61:1T(2012), pp. 293-297. [10.13182/FST12-A13435]

Availability:
This version is available at: 11583/2460583 since: 2020-11-01T19:00:25Z

Publisher:
American Nuclear Society

Published
DOI:10.13182/FST12-A13435

Terms of use:

This article is made available under terms and conditions as specified in the corresponding bibliographic description in the repository

Publisher copyright

(Article begins on next page)

02 December 2023

PROGRESS IN MULTI-PHYSICS MODELING OF INNOVATIVE LEAD-COOLED FAST REACTORS

R. Bonifetto, S. Dulla, P. Ravetto, L. Savoldi Richard and R. Zanino

Dipartimento di Energetica, Politecnico di Torino, c. Duca d. Abruzzi 24, 0129 Torino Italy

The status of the development of a coupled neutronic/thermal-hydraulic model for the stability and safety analysis of advanced lead-cooled fast fission reactors is presented.

I. INTRODUCTION

Lead-cooled Fast Reactors (LFRs) represent one of the six innovative reactor designs identified in the frame of the Generation IV [1] undertakings. Within the 6th European Framework Program (FP6), the ELSY project [2] aimed at the development of a preliminary, full-scale lead-cooled reactor design, see Fig. 1. Within the 7th Framework Program the research activities in the field of lead-cooled fast reactors are focused on the LEADER Project (Lead-cooled European Advanced DEmonstration Reactor), which is the main motivation for the present work.

The design of an innovative reactor, such as the LFR, requires stability and safety assessments to be performed in both operational and accidental transient conditions.

To this aim, the development of suitable numerical tools is required, in order to enlighten all the relevant neutronic and thermal-hydraulic phenomena involved and to analyze the multi-physics effects. The present research activity is focused on the development of a computational tool for the dynamic analysis of lead-cooled reactors, coupling neutronic and thermal-hydraulic phenomena. The code is foreseen to be adopted in the stability and safety analyses for LFR and is required to be optimized in order to allow parametric studies with an acceptable computational effort.

The main purpose of the paper is to report on the current status of development of a flexible and modular full-core coupled thermal-hydraulic (TH) and neutronic (NE) analysis for simulation of control- and safety-relevant transients in lead-cooled advanced fast reactors. For the NE part, the model will build on the experience of our group in the development of computational methods for the neutronic analysis of fission reactors, see e.g. Ref. 3. For the TH part, the model shall heavily rely on the experience of our group in the development of computational tools for the analysis of thermal-hydraulic transients in superconducting magnets for fusion reactors, see e.g. Ref. 4, which perhaps surprisingly present a certain number of analogies with the situation to be considered here, see Fig. 2.

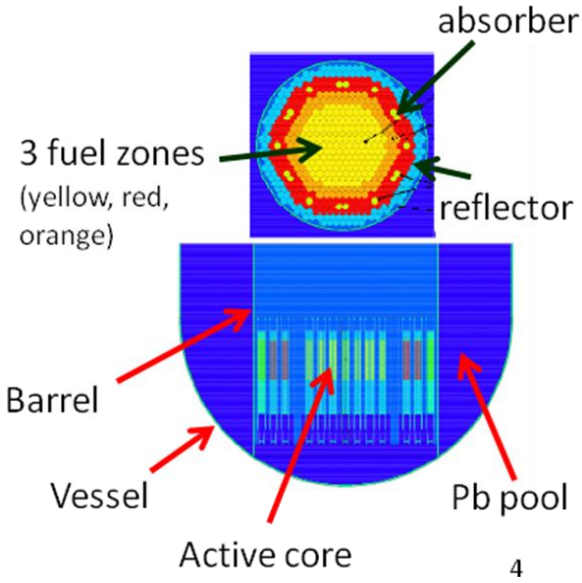

Fig. 1. Sketch of the ELSY reactor.

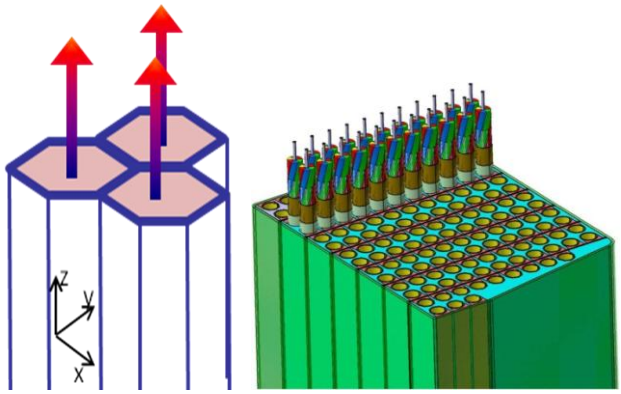

Fig. 2. Left: LFR core cross section showing a few FEs. Right: Cross section of an ITER TF coil [11].

II. MODEL DESCRIPTION

Our final target will be the development of a model for full-core geometry with homogenized hexagonal fuel elements (FE), see Fig. 3. As a first step, the neutronic and thermal-hydraulic modules have been developed for a single FE, in order to test the coupling strategy. As a consequence, the neutronic dynamic analysis can be carried out by a point model once the FE is homogenized by standard cross-section averaging procedures in energy and space.

II.A. Relevant time-scales

Several different time-scales are involved in the dynamics relevant for the analyses presented in this paper. Their separation will be used to justify the model assumptions adopted in the following.

The main NE time-scales are:

- Prompt neutron lifetime $\tau_p \sim 10^{-6}$ s
- Characteristic time for the evolution of the neutron spatial and spectral shape $\tau_{shape} \sim 10^{-4}$ s.
- Delayed neutron precursor lifetime $\tau_d \sim 10$ s

The main TH time-scales are:

- Pb-pin surface coupling $\tau_{Pb\text{-}pin} \sim 0.1$ s
- Pb transit along the FE $\tau_z \sim 1$ s
- Lead temperature (T_{Pb}) homogenization on a given FE cross section $\tau_{hom} \sim 1$ s, assuming uniform fuel temperature (T_{fuel}) on the same cross section
- Heat diffusion through wrapper $\tau_{xy} \sim 10$ s
- Pin temperature (T_{pin}) homogenization on a given pin cross section $\tau_{pin} \sim 10$ s.

II.B. Neutronic model

The space neutron kinetics will be described by a multi-group diffusion model adopting a coarse mesh approach (3D nodal scheme) for full-core evaluations in hexagonal geometry. The quasi-static method will be used for time integration, assuming that the neutron flux in the g-th energy group can be factorized as

$$\varphi_g = \psi_g(x, y, z; t) \cdot A(t), \qquad (1)$$

where A is the amplitude, evolving on a fast scale, and ψ_g is the shape, evolving on a slower scale. By a proper normalization of the shape function, the amplitude A can be assumed to be proportional to the effective thermal power as:

$$P(t) = P(t=0)A(t), \qquad (2)$$

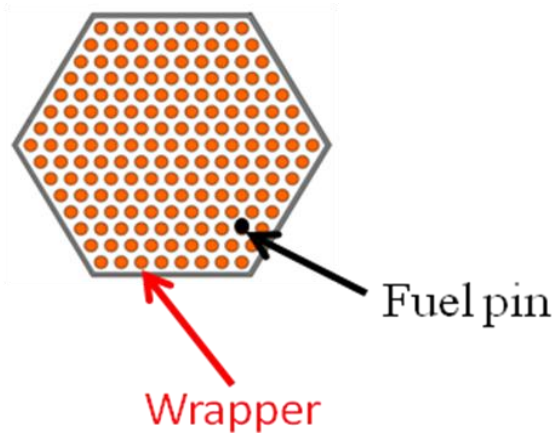

Fig. 3. Sketch of the hexagonal fuel element.

where $P(t=0)$ is the initial power.

In the present work we have implemented in the code a point kinetic model, which assumes ψ_g to be constant in time and the fission power axial distribution to be given by a cosine distribution. The evolution of the amplitude function is given by the following system of ODEs:

$$\begin{cases} \dfrac{dA(t)}{dt} = \left[\dfrac{\rho(t)-\beta}{\Lambda}\right]A(t) + \sum_{i=1}^{R}\lambda_i C_i(t) + S(t) \\ \dfrac{dC_i(t)}{dt} = -\lambda_i C_i(t) + \dfrac{\beta_i}{\Lambda}A(t) \qquad i = 1,\ldots,R, \end{cases} \qquad (3)$$

where Λ is the effective prompt neutron lifetime, β_i is the effective delayed neutron fraction for the i-th precursor family, and $\beta = \Sigma\, \beta_i$, λ_i the decay constant for the i-th family, C_i is the effective delayed neutron precursor concentration, and S is the effective external neutron source. The transient is driven by the reactivity ρ, which includes both external contributions (perturbations of the transport operator) and nonlinear feedback effects:

$$\rho(t) = \rho_{ext}(t) + \alpha_{fuel}\Delta T_{fuel}(t) + \alpha_{Pb}\Delta T_{Pb}(t), \qquad (4)$$

where α_{fuel} and α_{Pb} are the linear temperature feedback coefficients for the fuel and the coolant, respectively. In Eq. (3) we use the following values of the constants: R = 6, $\Lambda = 10^{-5}$ s, λ_i = (1.272×10^{-2}, 3.174×10^{-2}, 1.16×10^{-1}, 3.11×10^{-1}, 1.4, 3.87) s, β_i = (23.7, 122.7, 171.1, 262.7, 107.9, 45.1) pcm. The variations ΔT of the fuel and coolant temperatures are to be evaluated by the thermal-hydraulic model on the basis of the power distribution obtained by the solution of system (3).

II.C. Thermal-hydraulic model

The thermal hydraulic model approximates the (3D) problem in the full core geometry as a series of weakly coupled 1D problems along each FE. This approximation is justified by the fact that $\tau_{xy} >> \tau_{hom} \sim \tau_z$. Inside each FE, we assume on each cross section the uniformity of the coolant temperature $T_{Pb}(z)$ (which will be justified for timescales $\tau >\sim \tau_{hom}$) as well as of the fuel temperature $T_{fuel}(z) = \langle T_{pin}(r, z)\rangle$ (thanks to the relative uniformity of the heat source on each FE cross section); however, although $T_{pin}(r_{pin}, z) \approx T_{Pb}(z)$, since $\tau_{Pb\text{-}pin} << \tau_z$, we will have $T_{fuel}(z) \neq T_{Pb}(z)$, since $\tau_{pin} >> \tau_z$.

Here we shall present only the model for a single FE, which consists of the 1D balance of mass, momentum and energy, Eqs. (5)-(7), written for the lead pressure $p_{Pb}(z, t)$, velocity $v_{Pb}(z, t)$ and temperature $T_{Pb}(z, t)$, coupled to the 1D heat conduction model, Eq. (8), for the fuel temperature $T_{fuel}(z, t)$. These equations are basically the same reported in Ref. 5, except heat conductivity and buoyancy in lead have been added

$$\frac{\partial v_z}{\partial t} + v_z \frac{\partial v_z}{\partial z} + \frac{1}{\rho}\frac{\partial p}{\partial z} = -F v_z - g\cos\beta \quad (5)$$

$$\frac{\partial p}{\partial t} + \rho c_s^2 \frac{\partial v_z}{\partial z} + v_z \frac{\partial p}{\partial z} - \Phi \frac{\partial}{\partial z}\left(k\frac{\partial T}{\partial z}\right) + \rho c_s^{\,2} \frac{v_z}{A}\frac{\partial A}{\partial z} = \Phi\left[\frac{Q'}{A} + v_z \rho F\right] \quad (6)$$

$$\rho c_v \frac{\partial T}{\partial t} + \rho c_v v_z \frac{\partial T}{\partial z} + \rho c_v \Phi T \frac{\partial v_z}{\partial z} + -\frac{\partial}{\partial z}\left(k\frac{\partial T}{\partial z}\right) + \rho c_v \Phi T \frac{v_z}{A}\frac{\partial A}{\partial z} = \frac{Q'}{A} + v_z \rho F \quad (7)$$

$$\rho_F c_F \frac{\partial T_F}{\partial t} - \frac{\partial}{\partial z}\left(k_F \frac{\partial T_F}{\partial z}\right) = = \frac{\Pi_F H}{A_F}\left(T_F - T\right) + \frac{Q_{fuel}}{A_F} \quad (8)$$

where A is cross section, c_F is fuel specific heat, c_s is sound speed, c_v is Pb specific heat at constant volume, F accounts for friction effects, defined below, g is gravity acceleration, H is Pb-pin surface heat transfer coefficient, k is thermal conductivity, p is pressure, Π_F is perimeter, Q' is the linear heat flux exchanged between Pb and pins, Q_{fuel} is the linear power generation into fuel, T is temperature, v is velocity, z is the axial coordinate, β is the angle between z and vertical direction, ρ is density, Φ is Gruneisen parameter, defined below.

$$F = 2f\frac{|v_z|}{D_h} \quad (9)$$

$$\Phi = \left(\frac{\rho}{T}\frac{\partial T}{\partial \rho}\right)_s \quad (10)$$

where f is the friction factor and D_h is the hydraulic diameter.

The thermophysical properties of lead are taken for the time being from Ref. 6; this point will require further investigation because of some inconsistencies inside that set. The fuel thermophysical properties are presently those of UO_2, taken from Ref. 7. The friction factor for Pb and the heat transfer coefficient between Pb and pins are taken from correlations reported in Ref. 8 (results of these correlations agree within ± 10% with those of Ref. 9).

In the fuel energy balance the heat source term

$$Q_{fuel} = A_F E_f \Sigma_f \phi \quad (11)$$

where E_f is the energy produced per fission Σ_f is the macroscopic fission cross section and ϕ is the neutron flux, requires the coupling with the NE model.

II.D. Coupling between NE and TH models

Since $\tau_{shape} << \tau_z$, it is possible to couple the NE and the TH modules explicitly, alternating their solution on the slowest TH timescale. This is done using the TISC platform, [10] which calls each module in turn, exchanging at each TH time step the needed information (T_{fuel} and T_{Pb} from TH to NE, Q_{fuel} from NE to TH). This strategy, which we already tested [11] for different applications, works very well and allows each module to adopt the most suitable time stepping strategy, taking into account the respective time-scales.

III. A SIMPLE TEST CASE

In order to test the model, here we analyze a simple test case, in which a step reactivity of 100 pcm is inserted at time $t = 0$; this could correspond to, e.g., the ejection of a control rod.

III.A. Input definition

The assembly geometry and the following input data are taken from Ref. 2:

- $\alpha_{fuel} = -0.8$ pcm/K
- $\alpha_{Pb} = +0.35$ pcm/K

- Inlet T_{Pb} = 673 K
- Δp = 1.35 bar → v_{Pb} ~ 1 m/s
- Steady-state power (deposited only in the fuel): axial cosine shape, such that $\int q(z,t = 0)\, dz = P(t = 0) / N_{FE}$
- $P(t = 0)$ = 1500 MW_{th}
- N_{FE} = 433.

III.B. Results

The evolution of reactivity, power, maximum temperature of lead and fuel (T_{Pb}^{max} and T_{fuel}^{max}) following the reactivity insertion is reported in Fig. 4. The total reactivity of the system is brought back to zero by the effect of the negative feedback, which is compensating the external perturbation. For this type of configuration the system is therefore proven to be stable. The verification of stability is necessary in view of the fact that the temperature coefficient of the coolant is positive, although smaller in absolute value with respect to the fuel temperature coefficient. The stability follows from the combined temperature effects of fuel and coolant. The figure also confirms that, at least in this case, the maximum temperature of fuel and coolant remain well

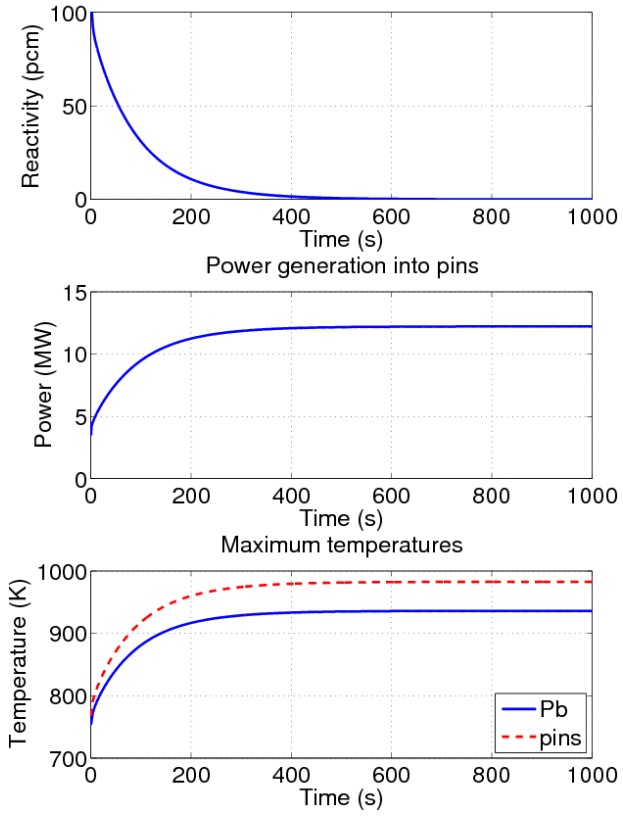

Fig. 4. Evolution of total reactivity, power and maximum temperatures for a transient induced by a 100 pcm reactivity insertion.

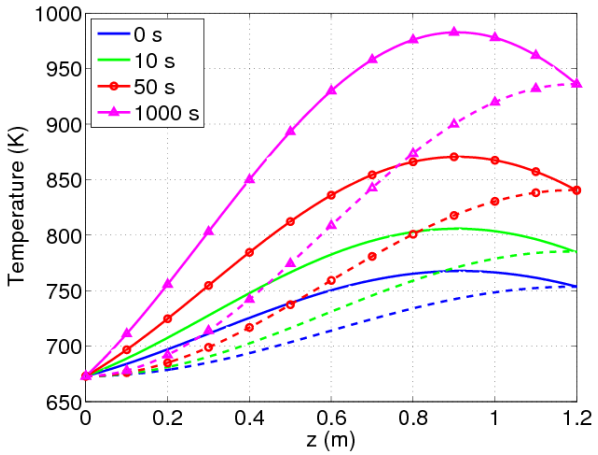

Fig. 5. Axial distribution of fuel and lead temperatures as a response to a 100 pcm reactivity insertion.

below the fuel melting temperature (T_{melt} ~ 3120 K, for UO_2) and the coolant boiling temperature (T_{boil} ~ 2016 K, for Pb), respectively.

The evolution of the spatial distribution of T_{Pb} and T_{fuel} is shown in Fig. 5. We notice the more symmetric profile of T_{fuel} responding directly to the cosine-distributed power input, while the more asymmetric profile of T_{Pb} is related to the advection in the lead coolant.

The evolution of the spatial distribution of the lead flow speed v_{Pb} is shown in Fig. 6. A higher value of Q_{fuel} leads to higher temperatures, therefore to lower values of the coolant density and impedance, which for a given Δp gives a higher velocity v_{Pb}. As the T_{Pb} increases (and the Pb density decreases) the flow accelerates along the channel, in order to maintain the constant mass flow rate.

Finally, we perform a study of the sensitivity of the predictions of the model to the value of α_{fuel}. This might

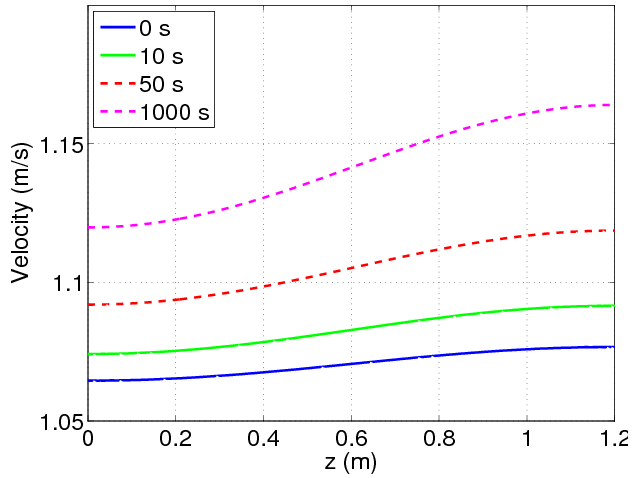

Fig. 6. Axial distribution of the coolant speed.

TABLE I. Effect of the fuel temperature coefficient.

Behavior			
increasing ρ = unstable			
decreasing ρ, Pb boiling			
stable			
α_{fuel} **(pcm/K)**		-0.3	-0.2

be of interest, e.g., while defining the Pu content in the MOX fuel; indeed, α_{fuel} may increase with increasing Pu content. Table I summarizes the results of the sensitivity study. As expected, it is seen that if α_{fuel} is larger than a certain threshold value α^*, the 100 pcm reactivity insertion leads to instability. The reason why $\alpha^* > -\alpha_{Pb}$ is that only the fuel is heated, therefore the reactivity becomes more sensitive to a temperature increase of the fuel than of the coolant. For values of $\alpha_{fuel} < \alpha^*$, the system goes through a transition region which is however still unacceptable, because T_{Pb}^{max} increases above T_{boil}, see Fig. 7.

IV. CONCLUSIONS AND PERSPECTIVE

A coupled TH and NE model has been developed for the case of a single adiabatic fuel element in a lead-cooled fast reactor. The model implements 1D conservation laws along the axial coordinate and a point kinetics method with a linear temperature feedback model.

The model has been applied to the study of a step reactivity insertion transient and the parametric effect of the fuel temperature coefficient has been presented.

As future work, the model will be extended from the single-assembly to the full-core level; this will be done implementing the coupling through different hexagonal assemblies in both the NE and the TH modules. The resulting computational tool should be applied to the study of safety transients and stability analyses.

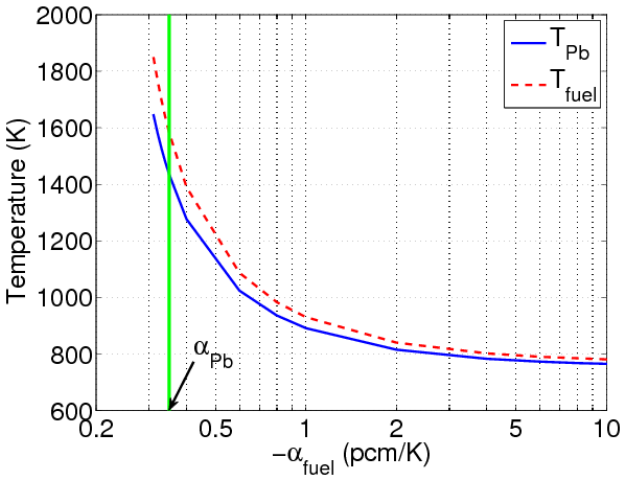

Fig. 7. Maximum fuel and coolant temperatures as a function of the value of the fuel temperature coefficient.

ACKNOWLEDGMENTS

This work has been partially supported financially by ENEA through the 2008-2009 Italian Ministry of Economic Development national research program on electric systems.

REFERENCES

1. "A Technology Roadmap for Generation IV Nuclear Energy Systems". GIF-002-00, USDOE Nuclear Energy Research Advisory Committee and the Generation IV International Forum (2002).
2. V. Sobolev, E. Malambu, H. Aït Abderrahim, "Definition of the ELSY core configuration parameters": Preliminary specifications for the ELSY-600 core, *EURATOM FP6 ELSY Project* (2007).
3. S. Han, S. Dulla, P. Ravetto, "Computational methods for multidimensional neutron diffusion problems", *Science and Technology of Nuclear Installations*, doi:10.1155/2009/973605 (2009).
4. L. Savoldi, R. Zanino, "M&M: Multi-Conductor Mithrandir Code for the Simulation of Thermal-Hydraulic Transients in Superconducting Magnets", *Cryogenics*, **40**, 179 (2000).
5. R. Zanino, S. De Palo, L. Bottura, "A Two-Fluid Code for the Thermohydraulic Transient Analysis of CICC Superconducting Magnets", *J. Fus. Energy*, **14**, 25 (1995).
6. "Handbook on Lead-Bismuth Eutectic Alloy and Lead Properties, Materials, Compatibility, Thermal-hydraulics and Technologies", OECD-NEA (2007).
7. S. G. Popov, J. J. Carbajo, V. K. Ivanov, G. L. Yoder, "Thermophysical Properties of MOX and UO_2 Fuels Including the Effects of Irradiation", ORNL Report TM-2000/351, November 2000.
8. N. E. Todreas, M. S. Kazimi, *Nuclear Systems*, vol.1, Hemisphere, New York (1993)
9. G. Bandini, et al., "CIRCE experimental set-up design and test matrix definition", ENEA Report IT-F-S-001, 28/02/2011.
10. TLK-Thermo GmbH, "TISC ® Connects simulation tools", available on http://www.tlk-thermo.com/
11. L. Savoldi Richard, F. Casella, B. Fiori, R. Zanino, "The 4C Code for the Cryogenic Circuit Conductor and Coil modeling in ITER**",** *Cryogenics*, **50**, 167 (2010).